Construction and Building Materials 27 (2012) 450–460

Contents lists available at SciVerse ScienceDirect

Construction and Building Materials

journal homepage: www.elsevier.com/locate/conbuildmat

Ionic transport in cementitious materials under an externally applied electric field: Finite element modeling

Yajun Liu [a], Xianming Shi [a,b,*]

[a] Corrosion & Sustainable Infrastructure Laboratory, Western Transportation Institute, Montana State University, P.O. Box 174250, Bozeman, MT 59717-4250, USA
[b] Civil Engineering Department, Montana State University, 205 Cobleigh Hall, Montana State University, Bozeman, MT 59717-3900, USA

ARTICLE INFO

Article history:
Received 8 February 2011
Received in revised form 26 June 2011
Accepted 18 July 2011
Available online 19 August 2011

Keywords:
Electrochemical chloride extraction
Finite element method
Chloride diffusion coefficient
Cement paste
Cement mortar
Concrete cracking
Numerical modeling

ABSTRACT

Rebar corrosion is a major deterioration mechanism for reinforced concrete and other cementitious materials, which is often resulted from the ingress of chloride ions from deicer applications or marine environments. Electrochemical chloride extraction (ECE) is an effective corrosion mitigation technique that is gaining world-wide application. In this work, accelerated migration tests with the aid of an externally-applied electric field were utilized to investigate chloride transport in cementitious materials, the results of which were inversely parameterized to extract chloride diffusion coefficients. Computational studies on transport of ionic species during ECE in cementitious paste, mortar, and concrete materials were then explored. The nonlinear partial differential equations to characterize spatial and temporal evolution of various species were formulated with the finite element method (FEM), and important factors for heterogeneous materials, such as ionic interactions between various species, chloride binding, role of aggregates and cracks, were discussed.

1. Introduction

Reinforced concrete is commonly used as an economical and durable construction material throughout the world. Owing to the high alkalinity in concrete, a thin and protective oxide/hydroxide film is normally formed on the surface of reinforcing steel bars during the service life of concrete structures [1,2]. Reinforced concrete, however, can often become contaminated with chlorides, as a result of exposure to deicing salt applications or marine environments [3,4]. Excessive accumulation of chloride ions at the rebar depth is detrimental to the longevity of concrete structures, which has been recognized as the most serious cause of premature deterioration and lead to a subsequent reduction in the strength, serviceability, and aesthetics of structures. Accordingly, the research of chloride ingress into concrete in salt-laden environments has received much attention over the past decades and the transport properties of chlorides in concrete have been considered critical to concrete durability [5–8].

The traditional repair method consists of replacing corrosion-damaged concrete with chloride-free concrete [9]. This temporary technique suffers from the need of removing sufficient chloride-containing materials from the structure of interest. Another technique known as electrochemical chloride extraction (ECE) has gradually gained acceptance as an effective method for non-destructive treatment of chloride-contaminated concrete structures to extend their service life [2,10–12]. ECE involves the application of a direct current of 1–5 A/m^2 between the reinforcing steel that acts as a cathode and an auxiliary anode towards which chloride ions are electrically driven [13]. The use of an external electric field has other advantages, such as realkalization of carbonated concrete, managing alkali–silica reaction by electrical injection of lithium ions into concrete, and mitigating rebar corrosion by electrical injection of corrosion inhibitors into concrete. With ECE, relatively large amounts of chloride ions can be removed from concrete within a relatively short time (a few weeks) [14]. As such, rebar corrosion will not reinitiate until either new chloride ions re-contaminate concrete or sufficient chloride ions migrate back onto rebar surface [15].

As a promising technique to treat chloride-contaminated concrete, ECE has not been widely adopted by the industry, partly due to the lack of detailed information on the underlying mechanisms. While there are studies on the transport of ions in concrete, such results are based on time-consuming and costly laboratory measurements. Existing experimental works on ECE are far from systematic and field data are often complicated by such factors as variations in bulk materials. It is envisioned that the limited experimental information should be coupled with theoretical

* Corresponding author at: Corrosion & Sustainable Infrastructure Laboratory, Western Transportation Institute, Montana State University, P.O. Box 174250, Bozeman, MT 59717-4250, USA. Tel.: +1 406 994 6486; fax: +1 406 994 1697.
E-mail address: xianming_s@coe.montana.edu (X. Shi).

0950-0618/$ - see front matter © 2011 Elsevier Ltd. All rights reserved.
doi:10.1016/j.conbuildmat.2011.07.019

modeling to improve the understanding of the transport behaviors of key ionic species in concrete during ECE. To this end, this work demonstrates the use of inverse parameterization and forward simulation of chloride transport during ECE, with the consideration of interaction between multiple ionic species, chloride binding with cement hydration products, and aggregate influence. Such numeric practices allow the amount of laboratory work to be significantly reduced while providing valuable insights for concrete rehabilitation.

2. Experimental

In order to cover a wide range of mix designs, cementitious paste and mortar samples with different amounts of fly ash and sand were prepared in this work, as detailed in Table 1. An ASTM C150-07 type II low alkali Portland cement (Ash Grove Montana City Plant, Clancy, MT) and an ASTM C618 class F fly ash (Jim Bridger Power Plant, Rock Springs, Wyoming) were utilized. For either cement or fly ash, no more than 34% of the particles can be retained on a 325-mesh (44 μm) sieve. A water/cementitious materials ratio of 0.40 was specified for all the mix designs. To investigate the effect of coarse aggregates on chloride diffusion, coarse aggregates with diameters from 10 to 20 mm were also utilized. The details of all the mix designs are presented in Table 1. For mortar samples, cement is mixed with water at a low speed hand mixer for 5 min. Subsequently, sand, sifted to allow a maximum size of 1.18 mm in diameter and prepared to reach the surface saturated dry (SSD) condition, was added as fine aggregates and the slurries were stirred for 3 min. All the slurries were cast into hollow plastic cylinders of 1.5 in. (38 mm) in diameter and 3 in. (76 mm) in length, and then carefully compacted to minimize the amount of entrapped air. The cylindrical samples were de-molded after curing for 24 h with over 90% relative humidity. After de-molding, the samples were cured with over 90% relative humidity for 28 days. With a low-speed saw equipped with a diamond blade, disk specimens measuring around 10 mm in thickness for 90–d old paste/mortar samples and 25 mm in thickness for 360–d old concrete samples were cut from the center of cylinders to minimize possible surface evaporation and air entrapment effects on specimen permeability. The sample thicknesses were chosen on the basis of two considerations. One is to have the thickness much greater than the maximum aggregate size in the sample so that the chloride penetration over the inhomogeneous sample matrix can be reasonably averaged to estimate the apparent chloride diffusion coefficient. The other is to have the thickness as thin as possible to allow the determination of chloride diffusion coefficient in a reasonably short duration. The cut surfaces of disk specimens were then polished using sandpapers with grit sizes from 400 to 800.

To perform electromigration tests, a two-compartment cell schematically shown in Fig. 1 was utilized. A disk specimen was sandwiched between two plastic compartments. Solution leakage between the plastic rim and the disk specimen was prevented by plastic washers and epoxy sealer. The two compartments and the disk specimen were tightened by a clamp mounted with nuts and bolts. Diffusion of ionic species in cementitious materials can be significantly affected by the amount of aqueous solutions in the pore space. Prior to migration testing, specimens should be fully saturated with water to minimize the influence of wick action (water transport) on the chloride penetration. To this end, the two compartments were filled with distilled water so that the specimens can be immersed for complete saturation. After 2 h, the distilled water in the cell was removed, and the left (source) chamber was filled with an electrolyte with 1 wt.% NaOH and 3 wt.% NaCl to simulate an aggressive environment, whereas the right (destination) chamber contained a 1 wt.% NaOH electrolyte. Once the sample disk and the electrolyte solutions were in place, a voltage of 30 V was applied through stainless steel electrodes immersed in the two compartments. A 100 Ω resistor was also incorporated into the electric circuit, the potential drop over which was periodically measured to monitor the change of electric current in the system. The chloride concentration in the right chamber has to be monitored in order to determine the flux of chloride, which was realized with the use of a custom-made Ag/AgCl chloride sensor. The chloride sensor was calibrated using NaCl solutions of known concentrations, before used for periodical reading of chloride concentration in the destination chamber. The temporal evolution of chloride sensor reading for various mix designs is collectively presented in Fig. 2.

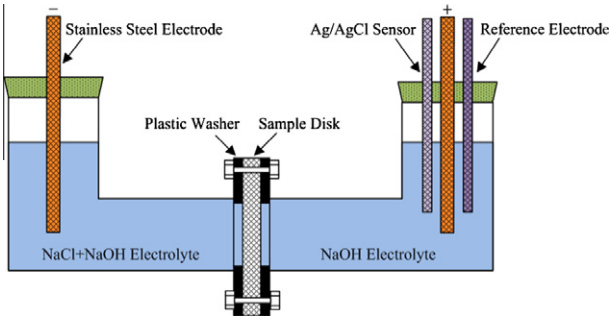

Fig. 1. Schematic drawing for the electromigration test setup.

3. Model description

3.1. Forward calculation

Cementitious materials (paste, mortar, or concrete) feature a relatively high level of porosity. When the pore structure and cracks are filled with water, the ions that penetrate into cementitious materials can be captured either physically or chemically. Chloride ions in concrete are either free or bound. The free ones are water-soluble and can attack the passive film on the rebar surface to initiate pitting corrosion, whereas the bound ones exist in the form of chloro-aluminates, making them unavailable for free transport. Chloride binding can remove free chloride ions from pore solutions, thereby slowing down the rate of penetration. In

Table 1
Mix designs and chloride diffusion coefficients evaluated in this work (all in weight fraction).

Mix ID	Cement	Fly ash (class F)	Sand/cementitious materials ratio	Critical parameters		Diffusion coefficients (10^{-11} m^2/s)	
				Thickness (mm)	t_0 (min)	Modified Nernst–Plank equation	Direct optimization
1	100	0	0	10.5	155	1.52	1.48
2	95	5	0	11.2	213	1.26	1.15
3	85	15	0	10.3	201	1.13	0.98
4	100	0	0.5	10.3	182	1.25	1.35
5	100	0	1	11.0	209	1.24	1.19
6	100	0	2	11.5	275	1.03	0.83
7	95	5	1	11.0	270	0.94	0.85
8	85	15	1	10.8	294	0.85	0.73
9	75	25	1	10.3	299	0.76	0.61
10	95	5	2	10.6	293	0.82	0.65
11	85	15	2	10.8	396	0.63	0.41
12	75	25	2	11.3	738	0.37	0.27
13[a]	100	0	0.6	25.4	36,378	0.0253	[b]
14[a]	75	25	1.9	25.4	44,896	0.0205	[b]

[a] The coarse aggregate/cementitious material ratio for mix design 13 and 14 are 2.2 and 2.8, respectively. The diameters for coarse aggregates are from 10 to 20 mm.
[b] The direct optimization technique is not utilized for mix design 13 and 14, as it is not practical to incorporate three-dimensional coarse aggregates into simulation domain.

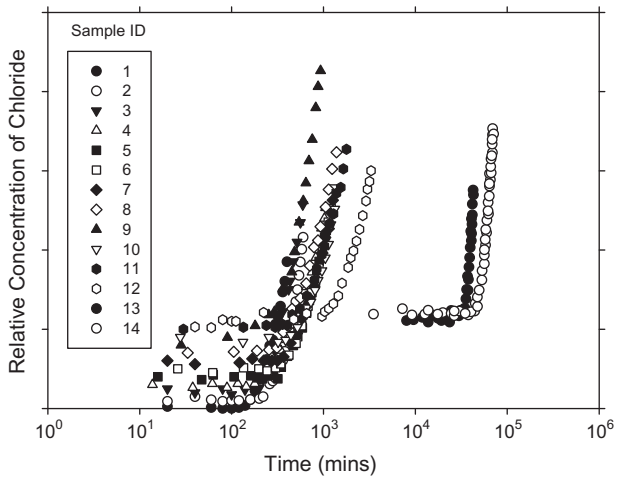

Fig. 2. Evolution of chloride concentration over time in the destination compartment during electromigration test. (Following the practice in Ref. [25], most chloride curves in this plot are vertically shifted to some degree in order to avoid overlap. The concentration scale for chloride is not given as this quantity is of no use in determining t_0^{meas}).

addition, minerals in cementitious materials can dissolve to a certain degree, making pore solutions an electrolyte with multiple ionic species. The flux of each species in the pore solution can be given by the following equation [16–21]:

$$J_i = -D_i \nabla C_i - \frac{D_i}{RT} C_i F Z_i \nabla \phi \tag{1}$$

where J_i, D_i, C_i, and Z_i are the flux, diffusion coefficient, concentration and valence number for species i in the pore solution, respectively; F is Faraday constant; R is gas constant, T is temperature; ϕ is electric potential.

For the transport of ions in a porous medium, one has to consider the influence of porosity as well as adsorption and desorption of ions. When these factors are taken into account, the law of mass conservation gives the following equation [21]:

$$p\frac{\partial C_i}{\partial t} + (1-p)\frac{\partial S_i}{\partial t} + \nabla \cdot (pJ_i) = 0 \tag{2}$$

where p is the porosity, and S_i is the concentration of bound ions of species i; t is time.

The mechanism of chloride binding is still debatable, and various empirical equations have been formulated, of which the following Langmuir isotherm is the most commonly used [22]:

$$S_{Cl} = \frac{\alpha C_{Cl}}{1 + \beta C_{Cl}} \tag{3}$$

where S_{Cl} and C_{Cl} are the concentration of bound and free chloride, respectively; α and β are materials properties.

Under an externally applied electrical field, all the ionic species in the pore solution contribute to the total electric current flux and thus affect the transport behavior of each other. The current density in the system of interest can be expressed by the following equation [14,21]:

$$i = pF\sum_{i=1}^{n} Z_i\left(-D_i\nabla C_i - \frac{Z_i F D_i}{RT} C_i \nabla \phi\right) \tag{4}$$

Based on the assumption that the electromagnetic signal travels more rapidly than ions in the solution, it is possible to use the following relation to calculate the electric potential ϕ [14]:

$$\nabla \cdot i = 0 \tag{5}$$

Inserting Eq. (4) in Eq. (5) leads to:

$$\nabla \cdot \left(pF\sum_{i=1}^{n} Z_i\left(-D_i\nabla C_i - \frac{Z_i F D_i}{RT} C_i \nabla \phi\right)\right) = 0 \tag{6}$$

which serves as a supplemental equation to link the electrical potential to the concentrations of various species.

In order to completely model a system, a set of boundary conditions for the concentration fields and electric field are mandatory. For boundary conditions to describe the evolution of species concentrations, invariant concentrations and fluxes can be specified by the following:

$$C_i = C_{i0} \tag{7}$$

$$-n \cdot J_i = J_{i0} \tag{8}$$

where C_{i0} is a user-defined value for the concentration of species i; J_{i0} is a predefined value for the flux of species i; n denotes the unit vector normal to the boundary. During the ECE process, hydroxyl ions are generated at the cathode, which follows:

$$2H_2O + 2e = 2OH^- + H_2 \tag{9}$$

Therefore, hydroxyl ions at the steel cathode can be assumed to have a flux proportional to the externally applied current density. Finally, the electric potential on the anode is set to zero and all the species other than hydroxyl ions have zero flux on the cathode. For boundary conditions to describe the evolution of electric field and current density, current flow and electric potential can be assigned as below:

$$-n \cdot i = i_0 \tag{10}$$

$$\phi = V_0 \tag{11}$$

where i_0 is the inward current density; V_0 is a predefined value for the electric potential.

3.2. Inverse parameterization

Inverse parameterization of chloride diffusion coefficients is gaining increasing importance in light of engineering demand to evaluate the service life of reinforced concrete structures. Traditionally, chloride diffusion coefficients can be experimentally obtained through two techniques, i.e., natural diffusion and accelerated electromigration. Inverse parameterization with natural diffusion is done by fitting chloride concentration profiles with the following analytical solution for a fixed surface concentration [23]:

$$c(x,t) = c_s\left(1 - erf\left(\frac{x}{2\sqrt{D_n t}}\right)\right) \tag{12}$$

where $c(x,t)$ is the distribution of chloride ions; c_s is the surface concentration of chloride; x is the spatial coordinate variable; D_n is the natural diffusion coefficient of chloride. However, evaluation of chloride diffusion coefficients with accelerated electromigration obeys the following equation [24]:

$$D_e = \frac{dRT}{t_0 zEF} \tag{13}$$

where d is the thickness of sample disk; t_0 is time required for chloride to penetrate sample disk; E is gradient of electric potential; z is the charge (1 for Cl^-); D_e is the chloride diffusion coefficient evaluated with accelerated electromigration. Natural diffusion tests are time-consuming, while an applied electric field can accelerate the transport of chloride ions so that the time taken for necessary measurements can be shortened from several months to a few days. Chloride diffusion coefficients from natural diffusion and acceleration tests take into account chloride binding implicitly. The treatment of chloride binding in a more accurate manner is essential

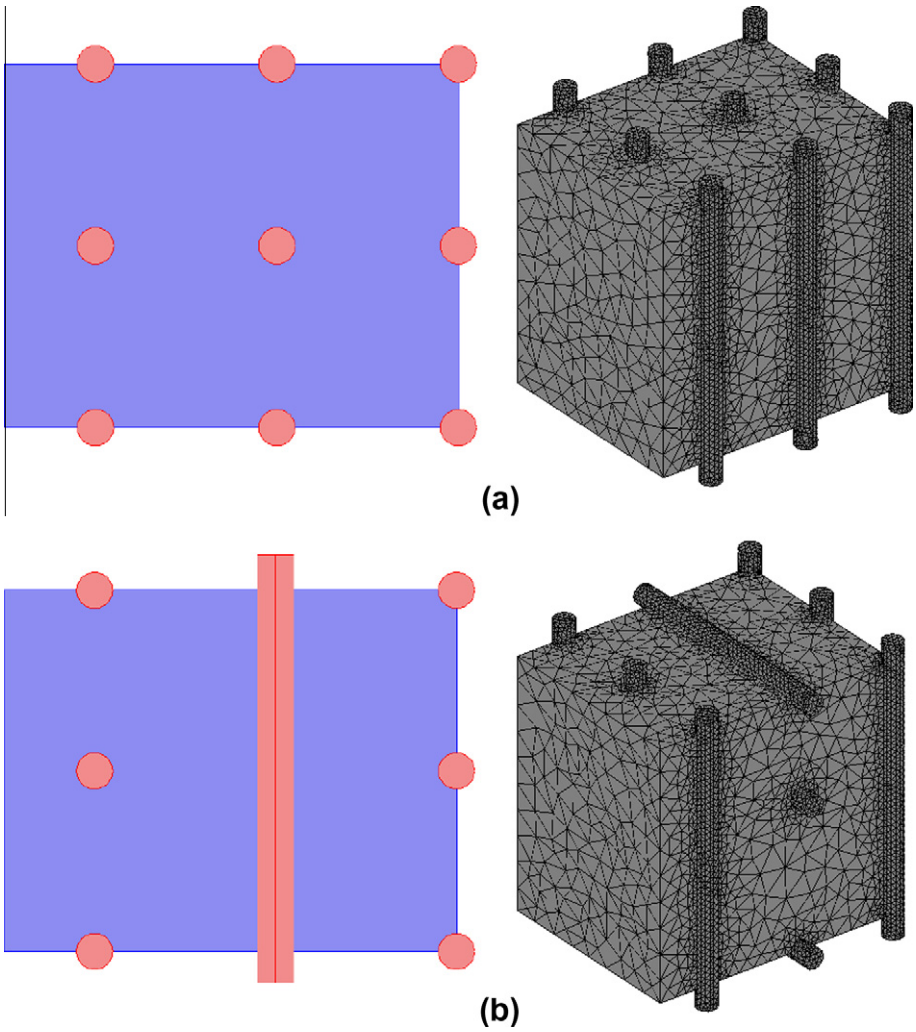

Fig. 3. Geometric setup and rebar arrangement for the simulation.

when those results are used to evaluate the initiation period of rebar corrosion and to predict the service life of concrete structures.

In this work, an inverse parameterization process that fully takes into consideration ionic interactions will be employed. This inverse parameterization has not been used for extracting chloride diffusion coefficients in the literature, which in fact can take the interaction of all the ions present into consideration. Frequently, the experiment has been conducted and the concentration of chloride ions around the cathode is measured as a function of time, but the diffusion coefficients for various species are not known *a priori*. A common way of treating inversion problems is to minimize an error norm defined as the discrepancy between the predicted t_0 of the forward problem and the measured data based on:

$$\Phi = [t_0^{meas} - t_0^{calc}]^2 \tag{14}$$

where Φ is the error norm; t_0^{meas} and t_0^{calc} are the measured and calculated penetration time, respectively. This function is always positive and can reach a global minimum for the parameters that reproduce the experimental results to the best possible extent.

Mathematically, inverse problems belong to the class of ill-posed problems, because their solutions do not satisfy the general requirements of existence, uniqueness and stability under small changes to the input data. For a stable inverse problem solution, one needs to account for the lower and upper bounds of the unknowns, and interactively regulates the stop criteria so that the solutions should describe the general features of the experimental results. There are several derivative-free optimization techniques to minimize the object function. The Nelder–Mead simplex search algorithm [25] was chosen due to its simple characteristics, which can perform the optimization by perturbing the inputs and works very well for scalar functions with several variables. To couple the forward calculation with Eqs. (1)–(11) and the inverse evaluation of model parameters to extract the chloride diffusion coefficients, the forward problem is packaged as a subfunction that can be called in the Nelder–Mead simplex search process with the model parameters as inputs and the penetration time as outputs. As a result, the error norm can be calculated and fed into the optimization routine. The detailed process to evaluate t_0^{meas} has been reported elsewhere [24]. It is noted that t_0^{calc} is determined in the optimization process in such a way that the obtained evolution of chloride concentration with longer time is regressed with a linear function, the extrapolation of which to the time coordinate is t_0^{calc}. All the calculations were conducted with COMSOL Multiphysics™, a FEM numeric package for multipurpose simulations.

4. Results and discussion

4.1. Establishment of diffusion coefficients

Porosity and tortuosity are two materials properties that significantly affect the transport behavior of chloride ions in heterogeneous materials. Porosity is commonly defined as the ratio of the

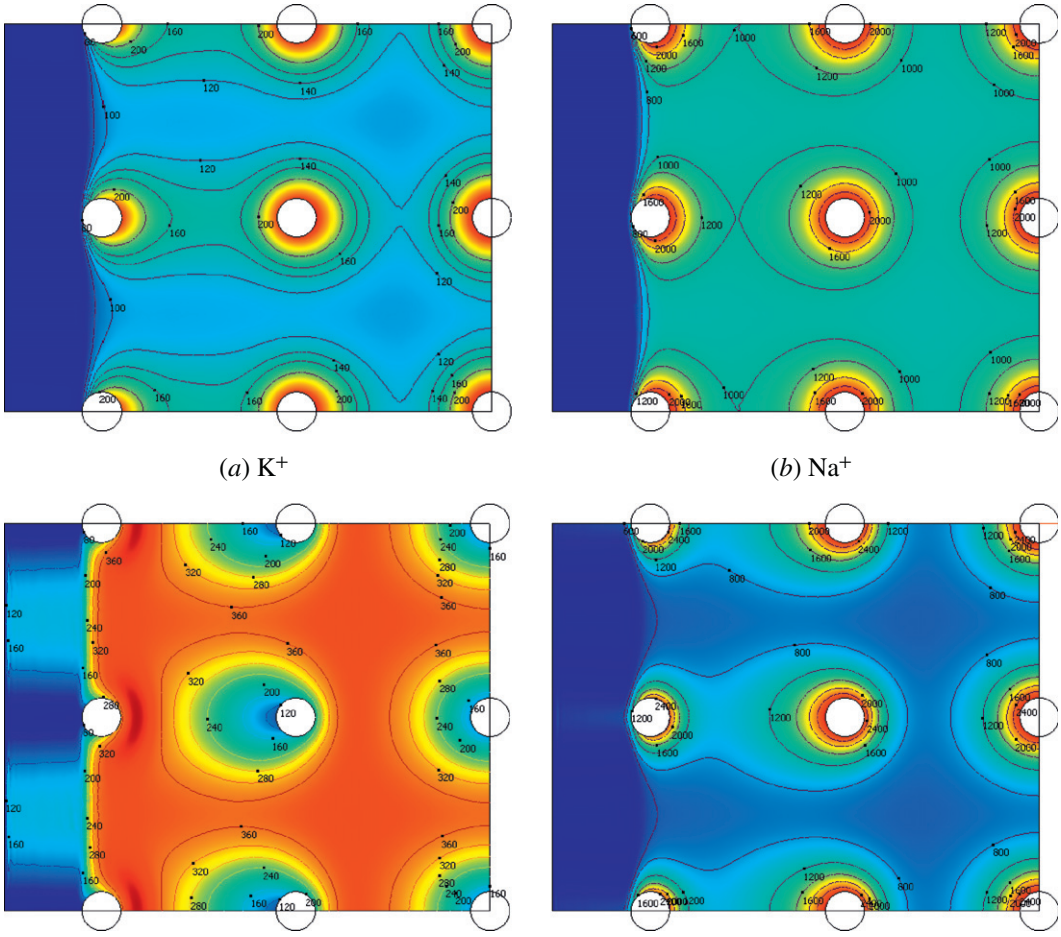

Fig. 4. Predicted concentration profiles of K^+, Na^+, Cl^- and OH^- ions after an ECE treatment of 1 A/m^2 for 8 weeks.

void space to the total material volume, which accounts for the total domain through which various ionic species can transport. However, porosity has no indication on the morphology features such as pore sizes and their distribution, which has been found to significantly influence the transport behavior of ionic species. Tortuosity, which refers to the ratio of the ionic diffusivity in an electrolyte to the diffusivity in the porous materials, characterizes the zigzagged nature of pores in the porous material. In cementitious materials, the water-to-cementitious-materials (*w/cm*) ratio generally dictates their porosity. The influence of porosity on the transport of ionic species in porous materials has been explicitly handed in Eq. (2). However, the influence of tortuosity is still implicit, which is reflected in the diffusion coefficients in Eq. (1). The pore structure in the mortar or concrete matrix is not uniform around the fine or coarse aggregates, owing to the formation of regions called interfacial transition zones (ITZs). In ITZs, porosity is significantly higher than the regions that are not in the vicinity of aggregates. When modeling the transport behavior in mortar or concrete materials, the effect of ITZs is reflected and incorporated into the diffusion coefficients. In other words, the experimentally obtained diffusion coefficients reflect averaged quantities over a larger scale.

To inversely parameterize the chloride concentration data obtained from electromigration tests (Fig. 2), one-dimensional simulation was first carried out with the given electric voltage (30 V in this case). Three major ionic species, Na^+, Cl^- and OH^- were considered in the pore solution. The boundary conditions at the anode were such that the concentration of each species has the same value as that in the aqueous electrolyte. For this specific case, the initial concentrations of Na^+, Cl^- and OH^- on the anode were 250, 0, and 250 mol/m^3, respectively. Furthermore, the initial concentration in the pore solution of salt-contaminated concrete prior to the treatment was assumed to be 750, 500, 250 mol/m^3 for Na^+, Cl^- and OH^-, respectively, which is consistent with the experiment design. When the chloride binding effect is considered explicitly in Eq. (2), the diffusion coefficients of various ionic species are mainly characterized by the tortuosity. As such, this constraint was assigned for Na^+, Cl^- and OH^- diffusion coefficients in the evaluation process. To achieve a better convergence, all the initial values for diffusion coefficients of Na^+, Cl^- and OH^- were set to be 10^{-11} m^2/s, which is the right order of magnitude for many ionic species. For Eqs. (2) and (3), the porosity and binding parameters were taken from Refs. [26,27], respectively. The diffusion coefficients of chloride obtained via the inverse parameterization and the Nernst–Plank equation in Eq. (13) for various mix design are presented in Table 1, where the chloride diffusion coefficients obtained using the two methods differ to some degree for any given mix design. In the subsequent computational studies, only mix design number 4 is adopted as an example.

4.2. Computational study of ECE

4.2.1. Distribution of ionic species after ECE

The initiation and propagation of rebar corrosion hinge on the relative concentration of aggressive chloride ions to protective hydroxyl ions. In reality, chloride ions act as catalyst for pitting

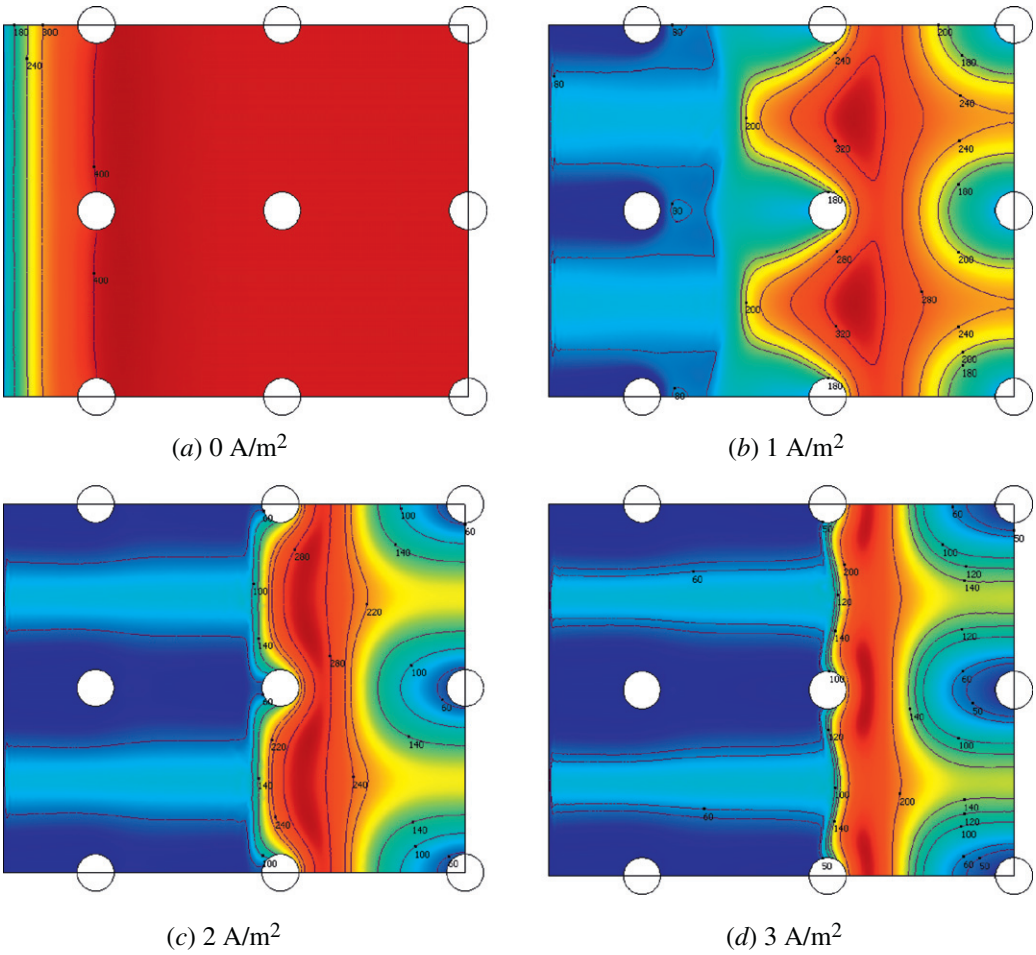

(*a*) 0 A/m^2 (*b*) 1 A/m^2

(*c*) 2 A/m^2 (*d*) 3 A/m^2

Fig. 5. Distribution of Cl^- ions after an ECE treatment of 0, 1, 2 and 3 A/m^2 for 24 weeks.

corrosion of steel once their concentration on rebar surface reach beyond a threshold level to disrupt the rebar passive film. Although the chloride threshold has been expressed as the free chloride concentration or the total chloride content by weight of concrete, the chloride-to-hydroxyl concentration ratio is a more acceptable criterion, as the competition of aggressive Cl^- and inhibitive OH^- governs the pitting/repassivation of steel. The geometric configuration, measuring 0.25 × 0.2 × 0.25 m, for the model setup is shown in Fig. 3a. In the simulation, the rebars are connected together in concept by specifying the same current density on rebar surface. The same action can also be done by using the same electric potential as boundary on the rebar surface. The initial conditions are such that the concentrations of K^+, Na^+, Cl^- and OH^- are 100, 900, 400 and 600 mol/m^3, respectively. Based on the three-dimensional modeling of ECE, the concentration profiles of K^+, Na^+, Cl^- and OH^- across the whole geometry domain are shown in Fig. 4, where the mortar material is subjected to a constant current density of 1 A/m^2 on the rebar surface for 8 weeks. Such two-dimensional plots are obtained through sectioning perpendicular to the rebar direction in Fig. 3a. Na^+ is mainly located around rebar domains, while K^+ is largely distributed between the rebar and the anode. The pattern for OH^- distribution is very similar to that of Na^+, as it is also mainly located around the rebar. The high concentrations of hydroxyl ions around the rebar, however, are caused by the generation of hydroxyl ions at the rebar surface through the electrochemical reaction following Eq. (9). In addition, the chloride removal can be clearly seen in Fig. 4c, in which the chloride concentration between the anode and the cathode features a low value while that behind rebars is found to be rather high. These results indicate that as the ECE treatment progresses, chloride and hydroxyl ions move gradually away from the cathode whereas potassium and sodium ions are attracted in the opposite direction. A high alkaline environment exists around rebar surface after ECE, resulting in pH values close to 14. Such a high level of hydroxyls is beneficial to protect rebar from corrosion, which in turn confirms that ECE is a very promising and effective technique in reducing chloride concentrations and increasing local hydroxyl concentration in the vicinity of rebars, which has been experimentally verified recently by Buenfeld et al. [14] and theoretically investigated by Wang et al. [21]. When an excess current density is applied on cathodes, hydrogen atoms generated can migrate within the steel and get trapped around defects [28,29]. Cracking of steel can thus occur around such locations at the macro-scale. It is generally believed that a small amount of hydrogen can lead to dramatic changes in material properties, and the increase in rebar strength enhances the susceptibility of hydrogen embrittlement for serious in-service problems, which is a common design concern with high strength steel [30].

4.2.2. Effect of current density on chloride removal

To investigate the effect of current density on the performance of ECE, concentrations of chloride are predicted with geometric configuration in Fig. 3a at four levels of current density for 24 weeks, i.e. 0, 1, 2, and 3 A/m^2. The naught current density corresponds to the natural diffusion in which no external current is imposed. The effect of current density on ionic transport is

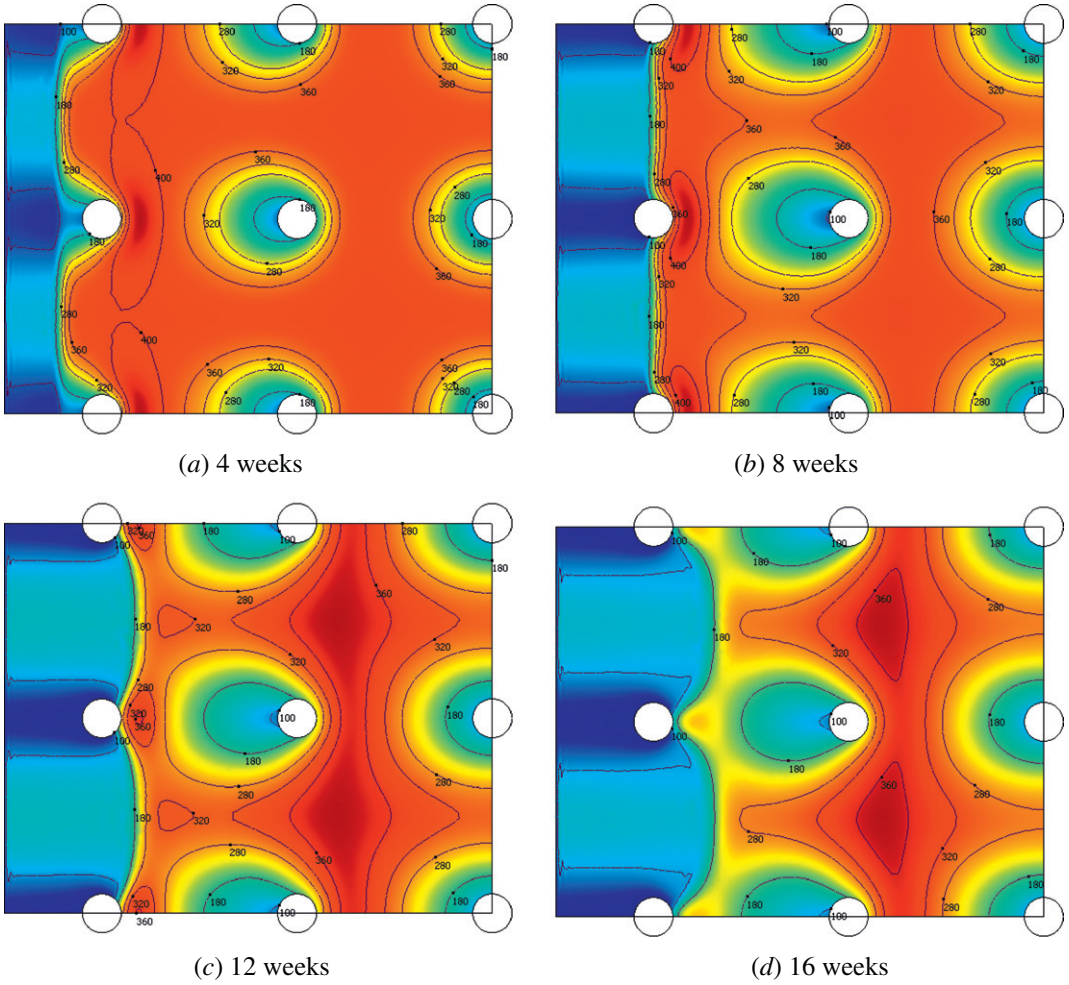

Fig. 6. Predicted chloride distribution after an ECE treatment of 1 A/m^2 for 4 weeks, 8 weeks, and 12 and 16 weeks, respectively.

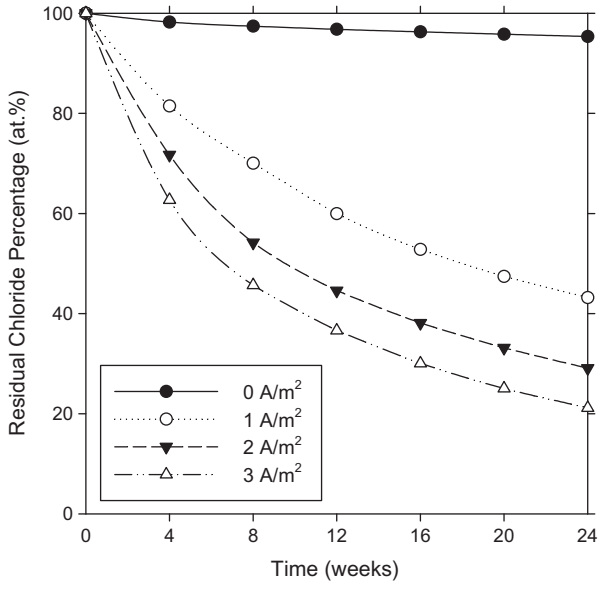

Fig. 7. Predicted variation of the residual chloride percentage with respect to the current density and treatment time.

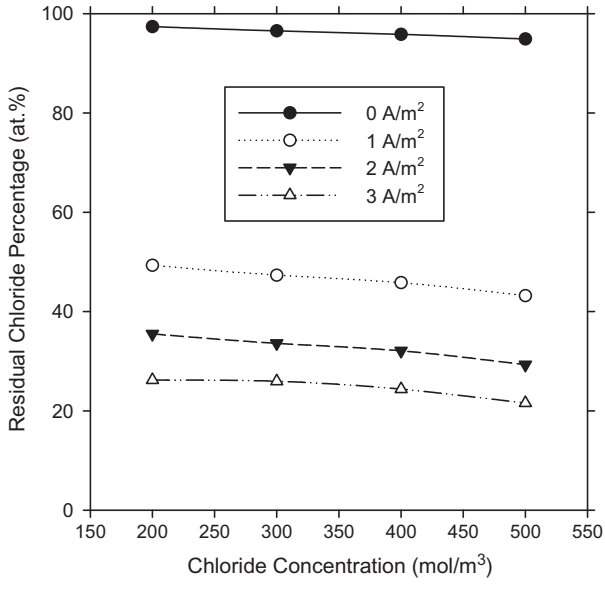

Fig. 8. Predicted effect of initial chloride content on the chloride removal for an ECE treatment of 24 weeks at various current densities.

explored by comparing the predicted concentration profiles of Cl^- values for different levels of current in Fig. 5. Based on the modeling results, natural diffusion of chloride to escape from material domain is the slowest process. Even after 24 weeks, almost 98% of the chloride ions still remain inside the concrete. With the current density of ECE treatment increasing, more chlorides are

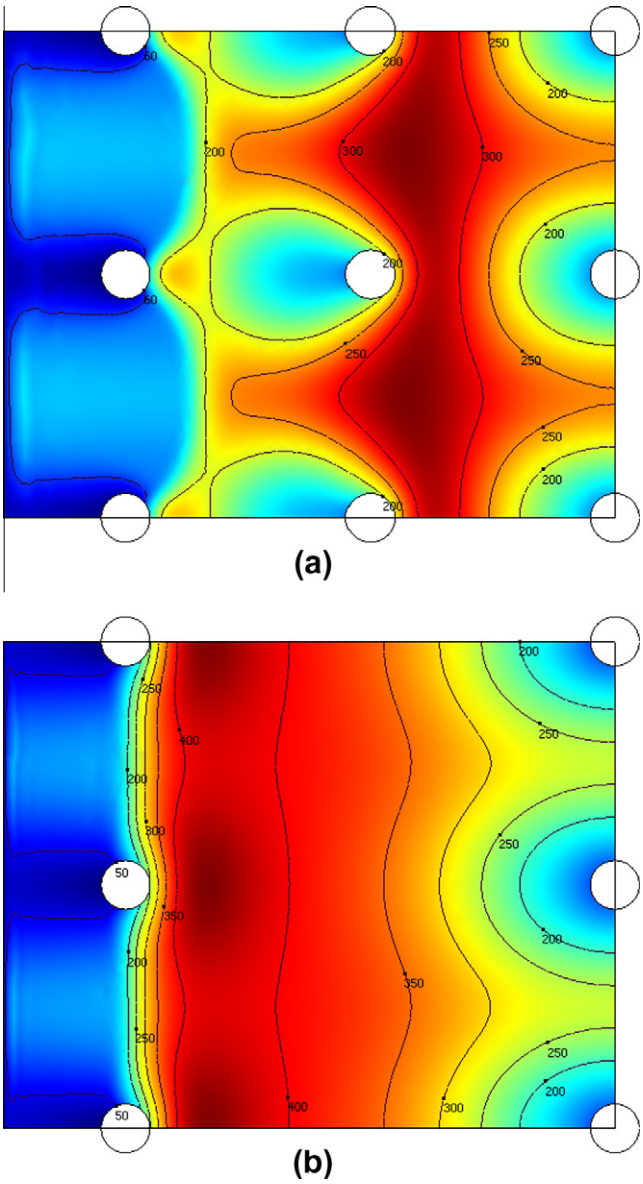

Fig. 9. Predicted chloride distribution for two kinds of rebar configuration after an ECE treatment of 1 A/m^2 for 20 weeks.

driven out. The residual chloride percentage after the ECE treatment for a certain time period is calculated by integration of the chloride concentration across the whole geometry domain and then divided by the initial chloride amount. It is interesting to note that the residual chloride percentage shows no significant improvement when the current density is raised from 2 to 3 A/m^2. Considering the potential detrimental effects of high current density on cement materials, a current density greater than 3 A/m^2 may not be beneficial for the overall performance of ECE treatment. Arya et al. [31] studied the effect of electric potential on ECE, and found the chloride removed increased with increasing electric potential, which is indirectly attributable to an increase in the current flow. The effect of current density has practical macro-structural implications. Once the current density is higher than 5 A/m^2, undesirable side effects such as chemical alternation and microstructure deterioration of the concrete matrix should be taken into consideration. Ihekwaba et al. [32,33] observed that the application of ECE significantly affected the interface mechanical properties of reinforced concrete, leading to a reduction in average bond strength. Such an effect may be attributable to the extraction of alkaline ions from the vicinity of cathodes, thus completely modifying the chemistry and phase morphology adjacent to the steel [34].

4.2.3. Effect of treatment time on chloride removal

The effect of treatment time on ionic transport is explored by comparing the model-predicted concentration profiles of free Cl^- after treatment for different durations from 4 to 16 weeks with a current density of 1 A/m^2 in Fig. 6, where extending ECE treatment time effectively removes chloride. After the treatment of 4 weeks, concentration changes of Cl^- ions are pronounced around the vicinity of rebars. As the treatment time is extended from 4 weeks to 16 weeks, the concentration of chloride near rebars surface drops significantly, which is consistent with the experimental observation by Arya et al. [31]. As shown in Fig. 6, the residual chloride percentage decreases with time. In other words, the longer the treatment time, the more chlorides are removed by ECE. To further investigate the temporal effect, the evolution of residual chloride percentage as a function of time at various current densities is given in Fig. 7. However, for the region behind the rebar, the ionic transport driven by the electric field is much slower. It should be noted that in the field practice, ECE treatment usually lasts no more than 8 weeks, as constrained by cost and other factors. In addition, the concrete resistance increases with the treatment time, making it more difficult to maintain the current density of ECE.

4.2.4. Effect of initial chloride content on chloride removal

Fig. 8 illustrates the residual chloride percentage as a function of initial chloride content and current density. The ECE simulation is performed for 24 weeks with current density varying from 0 to 3 A/m^2 and initial chloride concentration assigned from 200 to 500 mol/m^3. To maintain electroneutrality, corresponding amount of Na^+ is introduced into the initial conditions. As evidenced, the residual chloride percentage decreases slightly as the initial chloride concentration increases, the tendency of which is consistent with the experimental findings by Arya et al. [31] who concluded that the effect is likely attributable to an increase in the amount of free chlorides with increasing total chloride content. However, little effect on increasing hydroxyl is accompanied. Such a conclusion is obtained from comparing the predicted concentrations of free Cl^- and OH^- after 24 weeks with various current density treatments.

4.2.5. Effect of rebar position on chloride removal

The influence of rebar configuration on ECE is investigated with the two geometries in Fig. 3. For this purpose, the current density is maintained at 1 A/m^2 on the cathode for 20 weeks, and all the boundary conditions and initial conditions remain unchanged. Integration of the chloride concentration over the whole geometry is performed, and the residual chloride ions are found to be 56% and 74% for Fig. 9a and b, respectively, which is presumably caused by the alternated electric potential distribution. With portions of rebars positioned perpendicular to the rest, a greater majority of domain volume will be characterized by higher electric potentials. As such, the extraction of chloride ions towards external anode is strongly hampered. It should be noted that the concentrations of chloride and hydroxyl ions presented in Fig. 9, both sectioned at three quarters of the height in Fig. 3, are for the in situ ionic distributions. After ECE, their concentrations will evolve by the internal electric field and inhomogeneous distribution of ionic species. Considering the much higher diffusion coefficient of hydroxyl than chloride, the change of hydroxyls ion around rebar will be more significant than that of chloride ions at various critical locations in the vicinity of rebars, which sheds light on the long-term

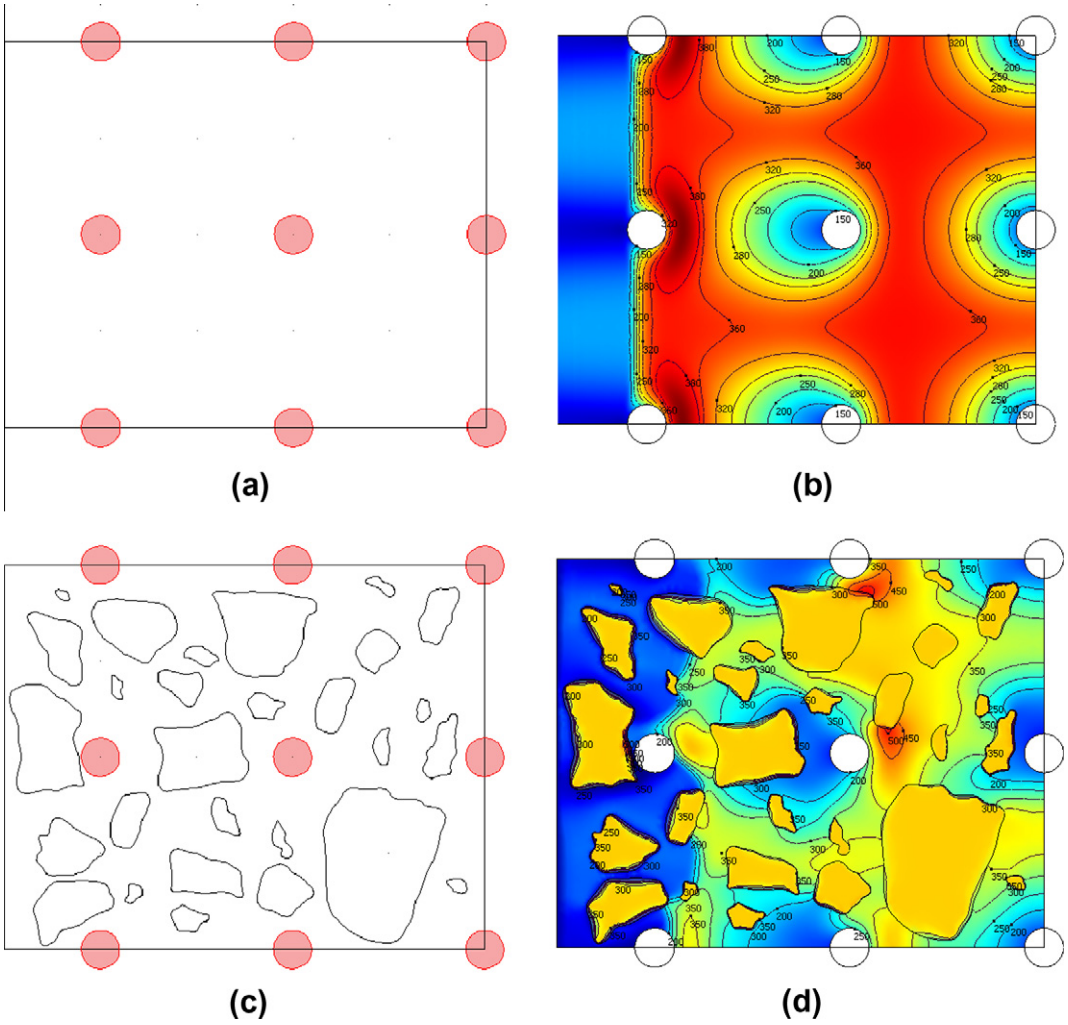

Fig. 10. Predicted aggregate effect on the chloride removal for an ECE treatment of 1 A/m^2 for 8 weeks.

implications for ECE. Although the ECE treatment of chloride-contaminated materials generally leads to lower chloride concentrations, higher pH values around rebar surface, and such implications are beneficial in terms of service life extension for reinforced concrete, the configuration of rebar will further complex the distribution of deleterious species and their extraction, which has been extensively discussed by Ihekwaba et al. [35] when they studied two sets of rebar configurations for ECE.

4.2.6. Effect of coarse aggregates on chloride removal

If coarse aggregates are added into mortar, the normal diffusion paths are partly blocked by these physical barriers, and the effective diffusion distance is thus longer than when there were no aggregates. Their effect depends on aggregate fraction, morphology and size distribution. In order to study a real concrete structure in ECE, FEM simulation is utilized for a heterogeneous concrete structure containing two phases, cementitious mortar and aggregates, to reveal the peculiarities of chloride diffusion in concrete. The domains of coarse aggregates are topologically extracted from real concrete structures. Such a process begins from tracing of coarse aggregates boundaries in a coordinate to be retained for the subsequent modeling, and the obtained boundary curves are fed into FEM model for aggregate domain construction. A simple two-dimensional and two-phase structure is constructed in Fig. 10, where a rectangular domain measuring 0.25 × 0.20 m is used, with its left surface exposed to a chloride-containing medium. To simulate aggregates, irregular domains with various diameters are randomly generated and distributed. ITZ zones feature a width of about 15 μm, and thus ITZ is treated with regions in which the porosity is about 40% higher that the bulk value [36]. Calculations are made for the case where the current density is maintained at 1 A/m^2 for 8 weeks. The final results are presented in Fig. 10, where a simulation for the control case is also presented. In reality, the aggregates within concrete are characterized by poor diffusivity due to their dense structures and thus great heterogeneities of ionic distribution in such a system are expected. In this simulation, the diffusion coefficient of ionic species in the aggregates was assumed to be 0.1% of that in the mortar phase. The residual chloride percentage increases with the incorporation of aggregates in Fig. 10, which is attributed to the barrier effect of aggregates. Both graphs clearly show that owing to the presence of aggregates, a smooth concentration surface across the domain from a homogeneous medium in Fig. 10b is now replaced with concentration bands with an undulating and gradually narrowing width in Fig. 10d. In a heterogeneous concrete, the ECE process appears to lag behind than that in its derived homogeneous medium. The great chloride diffusivity difference between aggregates and cement paste or mortar matrix remarkably complicates the ECE process for such a heterogeneous structure, which is confirmed by the significant difference in their diffusion coefficients shown in Table 1.

4.2.7. Effect of cracks on chloride removal

Cracks can be omnipresent in cement-based materials that are inherently brittle, which can compromise their strength and

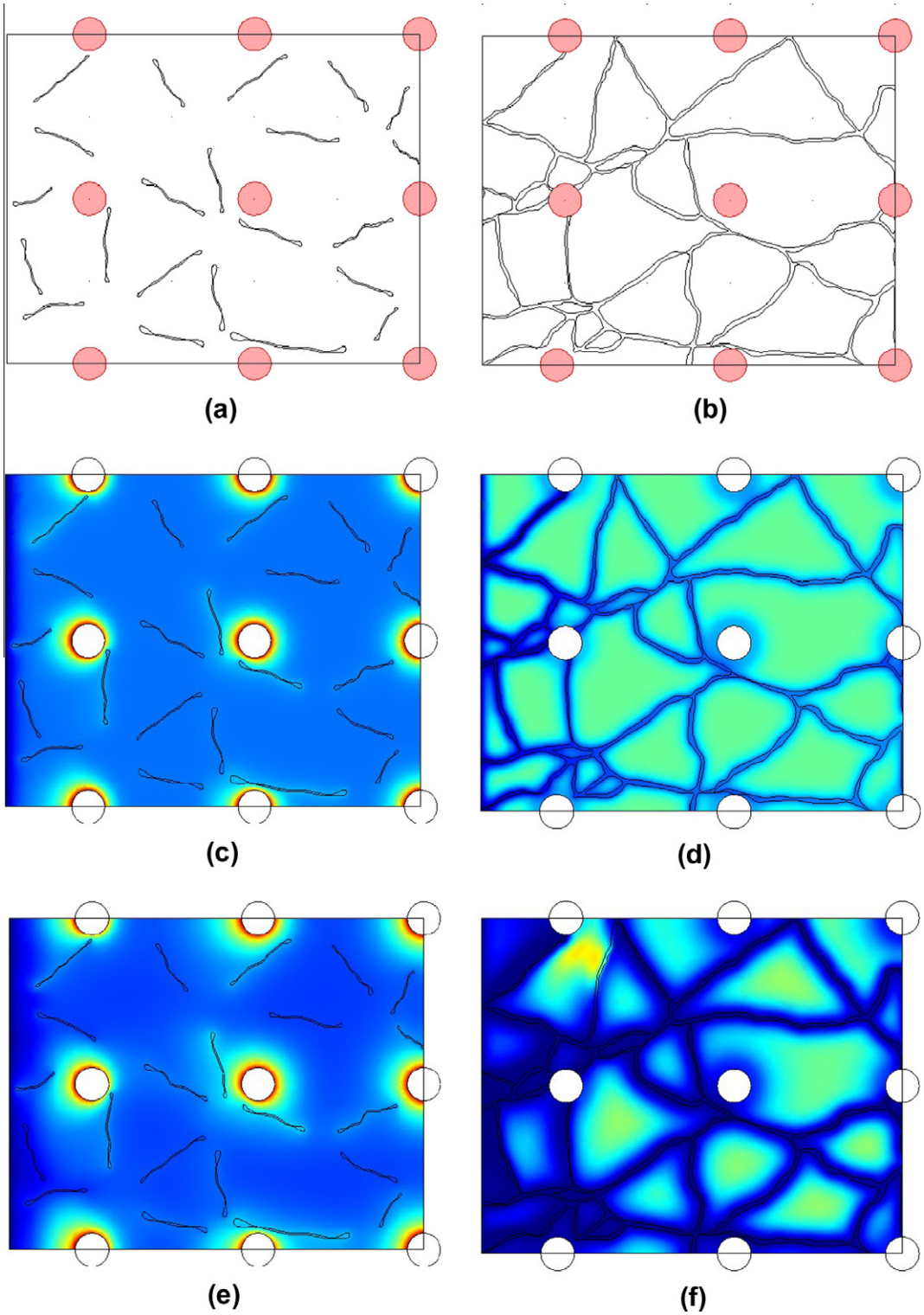

Fig. 11. Predicted crack effect on the chloride removal for an ECE treatment of 1 A/m^2 for 1 and 4 weeks, respectively.

durability properties. Microcracks often develop in cement-based materials as a result of mechanical loading (e.g., static or cyclic), environmental loading (e.g., freezing and thawing, rebar corrosion, alkali aggregate reactions, sulfate attack), and volumetric instability (e.g., shrinkage in fresh or hardened concrete, thermal contraction), and grow into macrocracks if not properly controlled. Such defects with appreciable sizes can have significant impact on the transport properties of cement paste, mortar or concrete, thereby undermining their durability characteristics. Once initiated, cracks facilitate the ingress of deleterious species (e.g., chloride ions) by creating preferential channels and pathways for them. Although this tendency has been universally recognized, consensus on reliable quantification is still lacking.

For the simulation purposes, mortar samples with two kinds of crack concentrations are taken into consideration in this work. The construction of domains for cracks follows the same procedure mentioned above for coarse aggregates. The domain size and rebar configuration are the same as used in Fig. 10. The simulation is

performed for 1 and 4 weeks with a current density of 1 A/m^2, respectively. Fig. 11a and b present the crack topologies, where discrete cracks and continuous cracks are provided. Compared with the chloride distribution in Fig. 11c and e with discrete cracks, ECE is more effective and pronounced for the simulation results in Fig. 11d and f. The chloride content in the cracked zone decreases with increasing crack size. The chloride concentration profiles along crack paths show more appreciable variation than those in the perpendicular direction. These suggest that the migration process under an externally-applied electric field perpendicular to the crack paths is considerably slower, and appears to be a limiting factor controlling the ECE process. It should be noted that this simulation was based on two-dimensional modeling and assumes uniformity of the cracks in the third direction. In real structures, it would be necessary to digitally characterize the three-dimensional distribution of the cracks as well as the aggregates before the simulation of species transport during ECE can be accurately conducted.

5. Conclusions

Two-dimensional and three-dimensional FEM models were developed to study the transport of ionic species in an externally applied electric field in cementitious samples. Electromigration tests were conducted for different mix designs, the results of which were utilized for inverse parameterization of diffusion coefficients necessary for model predictions. The forward calculation of the ECE process and inverse determination of the model parameters from relevant experimental data were presented. These two processes were integrated such that the model parameters obtained from the experimental results can be used to predict chloride removal under various conditions.

The distribution of ionic species in concrete after ECE was computationally studied. Na^+ and OH^- are found to be mainly located around the rebar, while K^+ is largely distributed between the rebar and the anode. The simulation also clearly illustrates the chloride removal as a result of ECE, with low chloride concentrations between the anode and the cathode and high chloride concentrations behind the rebar.

The effect of various factors on the performance of ECE was also predicted. Under the investigated situations, more chlorides are driven out of concrete with increasing current density and treatment time. With increasing initial chloride content, the residual chloride percentage decreases slightly. This study sheds light on the ECE performance and relevant factors, which provides guidance for practical applications. For example, a number of different types of positively-charged corrosion inhibitors can be electrically injected to embedded steel reinforcement at adequate concentration to provide corrosion protection. Likewise, positively charged pozzolanic nanoparticles can be driven into aged concrete under externally-applied electric field for crack healing, which is part of our planned future work.

Acknowledgements

The authors acknowledge the financial support provided by the Research & Innovative Technology Administration (RITA) at the U.S. Department of Transportation for this work. In addition, the help from Zhengxian Yang in preparing the cementitious samples is greatly appreciated.

References

[1] Fasjardo G, Escadeillas G, Arliguie G. Electrochemical chloride extraction from steel-reinforced concrete specimens contaminated by 'artificial' sea-water. Cem Concr Res 2002;32(2):323–6.
[2] Orellan JC, Escadeillas G, Arliguie G. Electrochemical chloride extraction: efficiency and side effects. Cem Concr Res 2003;34(2):227–34.
[3] Gjørv OE, Vennesland . Diffusion of chloride ions from seawater into concrete. Cem Concr Res 1979;9(2):229–38.
[4] Castellote M, Andrade C, Alonso C. Measurement of the steady and non-steady-state chloride diffusion coefficients in a migration test by means of monitoring the conductivity in the anolyte chamber comparison with natural diffusion tests. Cem Concr Res 2001;31(10):1411–20.
[5] Care S. Influence of aggregates on chloride diffusion coefficient into mortar. Cem Concr Res 2003;33(7):1021–8.
[6] Castellote M, Alonso C, Andrade C, Castro P, Echeverria M. Alkaline leaching method for the determination of the chloride content in the aqueous phase of hardened cementitious materials. Cem Concr Res 2001;31(2):233–8.
[7] Stanish K, Thomas M. The use of bulk diffusion tests to establish time-dependent concrete chloride diffusion coefficients. Cem Concr Res 2003;33(1):55–62.
[8] Tong L, Gjørv OE. Chloride diffusivity based on migration testing. Cem Concr Res 2001;31(7):973–82.
[9] Glass GK, Buenfeld NR. Chloride-induced corrosion of steel in concrete. Prog Struct Eng Mater 2000;2:448–58.
[10] Khatri RP, Sirivivatnanon V. Characteristic service life for concrete exposed to marine environments. Cem Concr Res 2004;34(5):745–52.
[11] Basheer L, Kropp J, Cleland D. Assessment of the durability of concrete from its permeation properties: a review. Constr Build Mater 2001;15:93–103.
[12] Marchand J, Samson E, Burke D, Tourney P, Thaulow N, Sahu S. Predicting the microstructural degradation of concrete in marine environment. In: Proceedings of the sixth CANMET/ACI international conference on durability of concrete; 2003. [SP-212:1127-1153].
[13] Mietz J, Elsener B, Polder R. Repair of reinforced concrete structures by electrochemical techniques-field experience. Corrosion of reinforcement in concrete-monitoring, prevention and rehabilitation, London; 1997. p. 125–40.
[14] Buenfeld NR, Glass GK, Hassanein Al M, Zhang J. Chloride transport in concrete subjected to electric field. J Mater Civ Eng 1998;10(4):220–8.
[15] Slater JE, Lankard DR. Electrochemical removal of chlorides from concrete bridge decks. Mater Perform 1976;15(11):21–6.
[16] Hassanein AM, Glass GK, Buenfeld NR. A mathematical model for electrochemical removal of chloride from concrete structures. Corrosion 1998;54(4):323–32.
[17] Amiri O, Ait-Mokhatar A, Dumargue P, Thouchard G. Electrochemical modeling of chloride migration in cement based materials Part I: theoretical basis at microscopic scale. Electrochem Acta 2001;46:1267–75.
[18] Gardner CL, Nonner W, Eisenberg RS. Electrodiffusion model simulation of ionic channels: 1D simulation. J Comput Electron 2004;3:25–31.
[19] Yu S, Page CL. Computer simulation of ionic migration during electrochemical chloride extraction from hardened concrete. Br Corros J 1996;31(1):73–5.
[20] Andrade C, Diez JM, Alaman A, Alonso C. Mathematical modeling of electrochemical chloride extraction from concrete. Cem Concr Res 1995;25(4):727–40.
[21] Wang Y, Li LY, Page CL. A two-dimensional model of electrochemical chloride removal from concrete. Comput Mater Sci 2001;20:196–212.
[22] Lu X, Li C, Zhang H. Relationship between the free and total chloride diffusivity in concrete. Cem Concr Res 2002;32(2):323–6.
[23] Gjorv OE, Tan K, Zhang M. Diffusivity of chlorides from seawater into high-strength lightweight concrete. ACI Mater J 1994;91(5):447–52.
[24] Yang Z, Shi X, Creighton AT, Peterson M. Effect of syrene–butadiene rubber latex on the chloride permeability and microstructure of Portland cement mortar. Constr Build Mater 2009;23:2283–90.
[25] Lagarias JC, Reeds JA, Wright MH, Wright PE. Convergence properties of the Nelder–Mead simplex method in low dimensions. SIAM J Opt 1998;9(1):112–47.
[26] Frias M, Rojas M. Microstructural alterations in fly ash mortars: study on phenomena affecting particle and pore size. Cem Concr Res 1997;27(4):619–28.
[27] Tang L. Chloride transport in concrete-measurement and prediction, Thesis, Chalmers University of Technology, Sweden, 1996.
[28] Woodtli J, Kieselbach R. Damage due to hydrogen embrittlement and stress corrosion cracking. Eng Fail Anal 2000;7(6):427–50.
[29] Thompsona AW. Current status of the role of hydrogen in stress corrosion cracking. Mater Sci Eng 1980;43(1):41–6.
[30] Oriani RA. Hydrogen embrittlement of steels. Annu Rev Mater Sci 1978;8:327–57.
[31] Arya C, Said-shawqi Q, Vassie PRW. Factors influencing electrochemical removal of chloride from concrete. Cem Concr Res 1996;26(6):851–60.
[32] Ihekwaba NM, Hope BB, Hansson CM. Pull-out and bond degradation of steel rebars in ECE concrete. Cem Concr Res 1996;26(2):267–82.
[33] Ihekwaba NM, Hope BB. Mechanical properties of anodic and cathodic regions of ECE treated concrete. Cem Concr Res 1996;26(5):771–80.
[34] Marcotte TD, Hansson CM, Hope BB. The effect of the electrochemical chloride extraction treatment on steel-reinforced mortar Part II: microstructural characterization. Cem Concr Res 1999;29:1561–8.
[35] Ihekwaba NW, Hope BB, Hansson CM. Carbonation and electrochemical chloride extraction from concrete. Cem Concr Res 1996;26(7):1095–107.
[36] Scrivener KL. The interfacial transition zone (ITZ) between cement paste and aggregate in concrete. Interface Sci 2004;12:411–21.